TABLE 1: Summary of reported cases of LCC*

Authors & Year	Age (yrs), Sex	No. of Cysts at Diagnosis	De Novo Cyst	Operation
Armstrong et al., 2009	21, F	multiple	yes	open surgical removal
Berry-Candelario et al., 2011	24, M	single	no	open surgical fenestration, CVP shunt
Brenner et al., 2006	20, F	multiple	no	
Briggs et al., 2008	8, M	single	yes	open surgical removal
	0.6, M	multiple	no	
Coeytaux et al., 2011	69, F	multiple	no	
Corboy et al., 2006	44, F	multiple	no	
Daglioglu et al., 2009	26, M	multiple	no	open surgical removal
Gulati et al., 2011	36, M	single	no	
Kaffenberger et al., 2009	59, F	multiple	no	open surgical removal
Kleinschmidt-Demasters et al., 2009	42, M	multiple	no	
	55, F	multiple	no	
	44, F†	multiple	no	
Labrune et al., 1996	11, F	single	yes	open surgical removal, stereotactic aspiration, ventriculoscopic fenestration, LP shunt, VP shunt
	8, F	multiple	no	open surgical fenestration, CSF shunt
	5, M	single	no	
Linnankivi et al., 2006	4, F			
	5, M			
	10, F	single or multiple	yes (in some cases)	
	20, F			
	43, M			
Marelli et al., 2008	27, F	multiple	no	open surgical removal
	45, M	multiple	no	open surgical removal
Nagae-Poetscher et al., 2004	12, M	single	no	
	9, F	single	no	
	14, F	single	no	
Sener et al., 2006	19, M	multiple	no	open surgical removal
Ummer et al., 2010	50, M	multiple	no	open surgical removal
Wargon et al., 2008	30, F	multiple	no	
present case	25, M	single	yes	open surgical removal, stereotactic aspiration, Ommaya reservoir

* CVP = cystoventriculoperitoneal; LP = lumboperitoneal; VP = ventriculoperitoneal.
† This case was previously reported by Corboy et al., 2006.

eration, the patient presented with left hemiparesis, and CT and MRI showed a de novo cyst in the right thalamus (Fig. 4). Stereotactic aspiration was performed without placement of an Ommaya reservoir because no cyst recurrence was observed after the previous 2 operations. However, contrary to our expectations, the cyst recurred 1 month after the third operation.

Fourth Operation. We performed stereotactic aspiration again and placed an Ommaya reservoir. Two weeks later, the cyst recurred and left hemiparesis again developed. We punctured the Ommaya reservoir and removed the viscous fluid.

Follow-Up. Two years after the last Ommaya reservoir puncture, serial CT images showed that the cysts in the left frontal lobe and right thalamus contained a small amount of fluid, while the other cysts remained decompressed. There were no symptoms related to the progression of the cysts. Additionally, no further de novo cyst formation was observed.

Discussion

In the present report, we describe the case of a patient with LCC who underwent surgery for repeated cyst formation. The first operation was performed to remove a large cyst and to obtain a histopathological diagnosis. The second and third operations were performed to decompress de novo cysts. The fourth operation was per-

formed to treat a recurrent cyst. In the cases reported to date (including the present one), 11 of 28 patients required surgery to treat progressively expanding cysts; we therefore conclude that surgery is often required in patients with LCC (Table 1).

The surgical strategies used in different patients varied and included open surgical removal, open surgical fenestration, stereotactic aspiration, ventriculoscopic fenestration, and CSF shunt placement.[1,2,4,7,9,11,13,15,16] However, the present case and previous reports highlight the possibility that LCC patients sometimes develop additional de novo cysts requiring surgery.[1,4,11,12] Therefore, less invasive and more repeatable procedures are worth considering when selecting surgical strategies. We felt that stereotactic aspiration would meet these criteria and chose it as an appropriate procedure for the treatment of de novo cysts.

Histopathologically, LCC is characterized by myelin loss, foci of rarefaction, gliosis, Rosenthal fibers, calcification, and excess increased water content,[6,9–11,16] which suggests the presence of secondary changes in the disruption of the blood-brain barrier following angioma-like microangiopathy.[6,9–12,14,16] Prominent angiomatous changes in the cyst wall and a high concentration of proteins in the cyst cavity may be conducive to cyst expansion. In such cases, a single stereotactic aspiration may be insufficient to resolve the cyst, and the placement of an Ommaya reservoir may allow the patient to avoid additional surgery.

Conclusions

The present report calls attention to the possibility of repeated cyst formation in patients with LCC and recommends the use of stereotactic aspiration with placement of an Ommaya reservoir. Open surgery may be necessary to remove cysts and confirm the histopathological diagnosis of LCC; however, stereotactic aspiration with Ommaya reservoir placement is considered to be a less invasive and more repeatable procedure for the treatment of repeated cyst formation in patients with LCC.

Disclosure

The authors report no conflict of interest concerning the materials or methods used in this study or the findings specified in this paper.

Author contributions to the study and manuscript preparation include the following. Conception and design: Ooba. Reviewed submitted version of manuscript: Hisamitsu. Approved the final version of the manuscript on behalf of all authors: Ooba. Administrative/technical/material support: Abe. Study supervision: Fujiki.

References

1. Armstrong MJ, Hacein-Bey L, Brown H: Cerebroretinal microangiopathy with calcifications and cysts: demonstration of radiological progression. **J Comput Assist Tomogr 33:**571–572, 2009
2. Berry-Candelario J, Kasper E, Eskandar E, Chen CC: Neurosurgical management of leukoencephalopathy, cerebral calcifications, and cysts: a case report and review of literature. **Surg Neurol Int 2:**160, 2011
3. Brenner C, Del Negro MC, Borigato EM, Miranda RV: Leukoencephalopathy with cerebral calcifications and cysts. **Neurology 66:**E32, 2006
4. Briggs TA, Abdel-Salam GM, Balicki M, Baxter P, Bertini E, Bishop N, et al: Cerebroretinal microangiopathy with calcifications and cysts (CRMCC). **Am J Med Genet A 146A:**182–190, 2008
5. Coeytaux A, Lobrinus JA, Horvath J, Kurian M, Vargas MI: Late onset of leucoencephalopathy with cerebral calcifications and cysts. **J Neuroradiol 38:**319–320, 2011
6. Corboy JR, Gault J, Kleinschmidt-DeMasters BK: An adult case of leukoencephalopathy with intracranial calcifications and cysts. **Neurology 67:**1890–1892, 2006
7. Daglioglu E, Ergungor F, Hatipoglu HG, Okay O, Dalgic A, Orhan G, et al: Cerebral leukoencephalopathy with calcifications and cysts operated for signs of increased intracranial pressure: case report. **Surg Neurol 72:**177–181, 2009
8. Gulati A, Singh P, Ramanathan S, Khandelwal N: A case of leukoencephalopathy, cerebral calcifications and cysts. **Ann Indian Acad Neurol 14:**310–312, 2011
9. Kaffenberger T, Valko PO, von Meyenburg J, Baráth K, Hewer E, Heppner FL, et al: A case of late onset leukoencephalopathy with cerebral calcifications and cysts in a 59-year-old woman. **Eur J Neurol 16:**278–281, 2009
10. Kleinschmidt-Demasters BK, Cummings TJ, Hulette CM, Morgenlander JC, Corboy JR: Adult cases of leukoencephalopathy, cerebral calcifications, and cysts: expanding the spectrum of the disorder. **J Neuropathol Exp Neurol 68:**432–439, 2009
11. Labrune P, Lacroix C, Goutières F, de Laveaucoupet J, Chevalier P, Zerah M, et al: Extensive brain calcifications, leukodystrophy, and formation of parenchymal cysts: a new progressive disorder due to diffuse cerebral microangiopathy. **Neurology 46:**1297–1301, 1996
12. Linnankivi T, Valanne L, Paetau A, Alafuzoff I, Hakumäki JM, Kivelä T, et al: Cerebroretinal microangiopathy with calcifications and cysts. **Neurology 67:**1437–1443, 2006
13. Marelli C, Savoiardo M, Fini N, Bartolomei I, Marliani AF, De Gonda F, et al: Late presentation of leucoencephalopathy with calcifications and cysts: report of two cases. **J Neurol Neurosurg Psychiatry 79:**1303–1304, 2008
14. Nagae-Poetscher LM, Bibat G, Philippart M, Rosemberg S, Fatemi A, Lacerda MT, et al: Leukoencephalopathy, cerebral calcifications, and cysts: new observations. **Neurology 62:**1206–1209, 2004
15. Sener U, Zorlu Y, Men S, Bayol U, Zanapalioglu U: Leukoencephalopathy, cerebral calcifications, and cysts. **AJNR Am J Neuroradiol 27:**200–203, 2006
16. Ummer K, Salam KA, Noone ML, Pradeep Kumar VG, Mampilly N, Sivakumar S: Leukoencephalopathy with intracranial calcifications and cysts in an adult: case report and review of literature. **Ann Indian Acad Neurol 13:**299–301, 2010
17. Wargon I, Lacour MC, Adams D, Denier C: A small deep infarct revealing leukoencephalopathy, calcifications and cysts in an adult patient. **J Neurol Neurosurg Psychiatry 79:**224–225, 2008

Manuscript submitted January 30, 2013.
Accepted May 16, 2013.
Please include this information when citing this paper: published online June 21, 2013; DOI: 10.3171/2013.5.PEDS1328.
Address correspondence to: Hiroshi Ooba, M.D., Ph.D., 1-1 Idaigaoka, Yufu, Oita, Japan 879-5593. email: ohba@oita-u.ac.jp.

Endocrine
DOI 10.1007/s12020-013-0046-4

ORIGINAL ARTICLE

The clinical and pathological significance of nitric oxide synthase in human pituitary adenomas: a comparison with MIB-1

K. Onishi · T. Kamida · Y. Momii · T. Abe · M. Fujiki

Received: 2 July 2013 / Accepted: 22 August 2013

Abstract The purpose of the present study was to define the clinical and pathological significance of nitric oxide synthase (NOS) in human pituitary adenomas, and to compare these values with those of the MIB-1 labeling index (LI) using an immunohistochemical method. Tissue specimens from 82 cases of surgically-treated pituitary adenomas were immunostained for hormone production for the MIB-1 LI and for the three NOS isoenzymes and five normal pituitary glands were immunostained for the three NOS isoenzymes as a control. The correlation between the clinical variables (age, functional status, tumor size, Hardy's grading, cavernous and/or sphenoid invasiveness, and progression) and mean MIB-1 LI, or between the same clinical variables and NOS immunoreactivity (IR) were analyzed. There was a statistically significant difference in the MIB-1 LI between macroadenomas and microadenomas, and between invasive adenomas and noninvasive adenomas. On the other hand, there was a statistically significant difference in the inducible NOS (iNOS) IR between invasive adenomas and noninvasive adenomas. Furthermore, the iNOS IR had a significant correlation with the MIB-1 LI. Invasive adenomas have a higher iNOS IR, and this correlated with the MIB-1 LI. These findings may be due to the function of iNOS, which plays an important role in tissue injury and repair.

K. Onishi · T. Kamida (✉) · Y. Momii · T. Abe · M. Fujiki
Department of Neurosurgery, Faculty of Medicine, Oita University, 1-1 Idaigaoka, Hasama-machi, Oita 879-5593, Japan
e-mail: kamida@oita-u.ac.jp

Keywords Nitric oxide synthase · MIB-1 labeling index · Pituitary adenomas

Introduction

Nitric oxide (NO) has been identified as a source of free radical oxidants in relation to the physiological and pathological events in the nervous system. NO is generated from L-arginine and molecular oxygen by three NO synthase (NOS) isoforms, named for the tissue in which they were originally described. Neuronal NOS (nNOS) was identified in the central nervous system, and is highly expressed in the cerebellum. Inducible NOS (iNOS) was first identified in inflammatory cells, such as monocytes, macrophages, and neutrophils, and endothelial NOS (eNOS) was discovered in the endothelial blood vessels [1].

Recently, it was reported that NO is involved in the regulation of the blood flow and the release of pituitary hormones [1–9]; however, the reports have been limited, and the role of NO in pituitary adenomas remains unclear. Furthermore, there has been no report of the relationship between NO and the progression of pituitary adenomas.

Although pituitary adenomas are commonly benign tumors, they are sometimes progressive and invade the surrounding tissues. The MIB-1 labeling index (LI), a marker of cellular proliferation, has been extensively studied in the progression of pituitary adenomas.

The purpose of the present study was to examine the clinical and pathological significance of NOS in the progression of human pituitary adenomas, and to compare it with the MIB-1 LI using an immunohistochemical method.

Published online: 06 September 2013

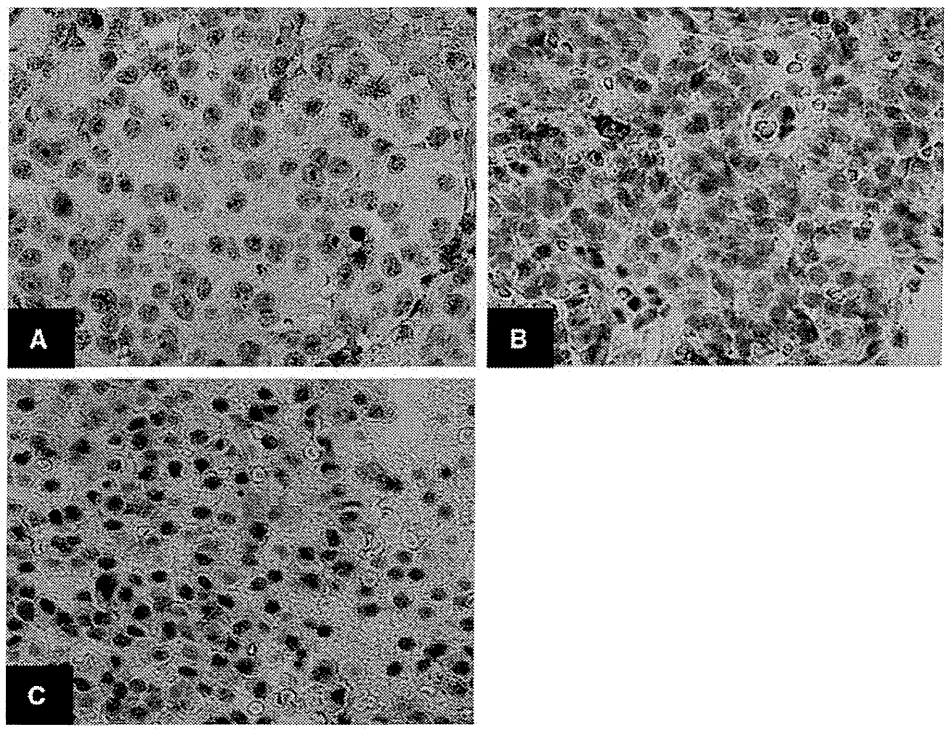

Fig. 1 **a** nNOS-positive GH-secreting adenoma cells, with a NOS immunoreactivity (IR) grading of 2 (×400). **b** iNOS-positive nonfunctioning adenoma cells with a NOS IR grading of 2 (×400). **c** eNOS-positive GH-secreting adenoma cells with a NOS IR grading of 2 (×400)

Methods

Normal human pituitary gland and pituitary adenoma samples

Eighty-two pituitary adenoma tissues (from 31 males and 51 females) were obtained during surgery from 2000 to 2012 at Oita University Hospital (Oita, Japan), and five normal human adenohypophyses were obtained during an autopsy from five patients without endocrine dysfunction, and were used as controls. The tumors included 16 growth hormone (GH)-producing adenomas, 12 prolactin (PRL)-producing adenomas, six adrenocorticotropic hormone (ACTH)-producing adenomas, and 49 non-functioning adenomas. The tumor size (macroadenomas: ≥10 mm in diameter, microadenomas: <10 mm in diameter), Hardy's grading (A; symmetrical extension to the suprasellar cistern, B; symmetrical extension to the recessed third ventricle, C; symmetrical extension to the whole anterior third ventricle, D; intracranial intradural parasellar extension, E; lateral cavernous invasion), and the invasiveness into the cavernous sinus and/or sphenoid sinus were defined on the basis of preoperative magnetic resonance imaging (MRI).

Table 1 Clinical and pathological characteristic of 82 pituitary adenomas used for immunohistochemistry

	Case	Tumor size		Hardy's grading		Invasiveness	
		Macro	Micro	A, B	C, D, E	Invasive	Non invasive
Patients (n, %)	82	74 (90.2)	8 (9.8)	33 (44.6)	41 (55.4)	20 (24.4)	62 (75.6)
Gender (n, %)							
Male	31	30 (96.8)	1 (3.2)	12 (40)	18 (60)	6 (19.4)	25 (80.6)
Female	51	44 (86.3)	7 (13.7)	21 (47.7)	23(52.3)	14 (27.5)	37 (72.5)
Clinical diagnosis							
Nonfunctioning	49	49 (100)	0 (0)	18 (36.7)	31 (63.3)	14 (28.6)	35 (71.4)
Acromegaly	16	12 (75)	4 (25)	7 (58.3)	5 (41.7)	1 (6.3)	15 (93.7)
Cushing's	6	3 (50)	3 (50)	3 (100)	0 (0)	0 (0)	6 (100)
Prolactinoma	11	10 (90.9)	1 (9.1)	5 (50)	5 (50)	5 (45.4)	6 (54.6)

Immunohistochemistry

All specimens were fixed in 10 % buffered formalin, routinely processed, paraffin-embedded, and cut into 3 μm sections. In addition to hematoxylin and eosin (H&E) staining, all tumors were immunostained for the full spectrum of pituitary hormones (ACTH, GH, and PRL; Dako Cytomation, CA, USA), thyroid stimulating hormone (TSH), luteinizing (LH) (Spring Bioscience, CA, USA), follicle-stimulating hormone (FSH) (Novocastra, Newcastle upon Tyne, UK), and MIB-1 (Dako Cytomation, CA, USA) and for the three NOS isoenzymes; nNOS (CHM, CA, USA), iNOS (BOX, CA, USA), eNOS (ABR, CO, USA) using the labeled streptavidin–biotin method.

The MIB-1 LI was determined by counting the number of positive cells in a total of 500–1,000 tumor cells observed in the highest staining regions of 10 high-power fields (×400). The results were expressed as the percentage of tumor cells with positive nuclei.

Data analysis

The NOS immunoreactivity (IR) of the analyzed antibody was scored independently by two observers who didn't know which NOS was stained, and they graded arbitrarily from 0 to 3 according to the proportion of cells stained. A value of 0 indicated the absence of staining, 1 indicated sporadic staining, 2 indicated heterogeneous staining and 3 indicated staining of the majority of the cells examined. The presence of a granular brown reaction product located in the cytoplasm of adenomas and endothelial cells was taken as a positive response (Fig. 1).

The correlation between the mean MIB-1 LI and clinical variables (age, functional status, tumor size, Hardy's grading, cavernous and/or sphenoid invasiveness, and progression) was analyzed by the Mann–Whitney U test. The correlation between NOS IR and the clinical variables was analyzed by the Chi square test. The progression was investigated in 11 patients who could be followed with MRI for more than 1 year after or before the operation. The progression was defined as volume growth by more than 5 % in 1 month. The correlation between the MIB-1 LI and NOS IR was analyzed by the Spearman correlation test. A value of $P < 0.05$ was considered to be significant.

Results

The clinical and pathological characteristics of the 82 pituitary adenomas used for immunohistochemistry are shown in Table 1. Most of the cases were macroadenomas, the majority of which were nonfunctioning adenomas and prolactinomas. The nonfunctioning adenomas and prolactinomas tended to be more invasive than the other tumors.

Figure 2 shows the MIB-1 LI in the pituitary adenomas according to the clinical diagnosis. The tumors with a MIB-1 LI > 1.0 % were all nonfunctioning adenomas and prolactinomas. Figure 3 shows the NOS IR in the pituitary adenomas according to the clinical diagnosis. Many nonfunctioning adenoma and acromegaly cases expressed nNOS, iNOS and eNOS IR, which was stronger than grade 2 compared with the other tumor types and control cases. Nonfunctioning adenomas had especially strong iNOS IR.

The mean MIB-1 LI had no significant associations with the age, functional status, Hardy's grading or progression (Table 2). On the other hand, there was a statistically significant difference in the MIB-1 LI between macroadenomas and microadenomas ($P < 0.05$), and between invasive adenomas and noninvasive adenomas ($P < 0.05$) (Table 2).

In the comparison between the NOS IR and clinical variables, there was a statistically significant difference

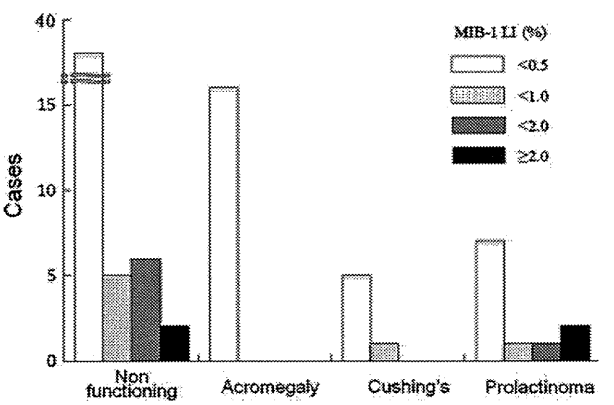

Fig. 2 The distributions of the MIB-1 LI in the pituitary adenoma cases

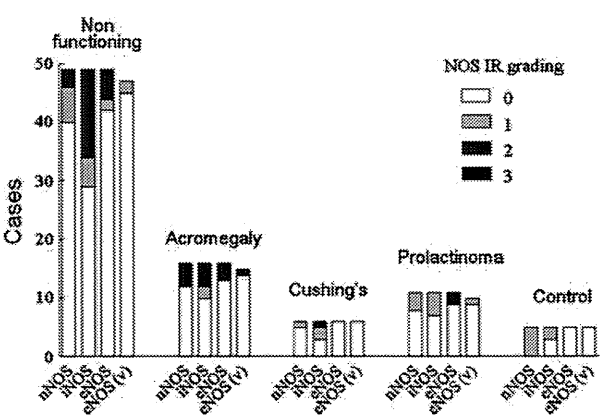

Fig. 3 The distributions of the NOS immunoreactivity (IR) in the pituitary adenoma cases. nNOS: neuronal NOS, iNOS; inducible NOS, eNOS; endothelial NOS, eNOS(v); endothelial cell eNOS

Table 2 Comparison between mean MIB-1 LI and clinical variables

Variable	Variable groups	Cases	MIB-1 LI (% ± SEM)	*P* value Mann–Whitney
Age(years)	≤45	19	0.35 ± 0.16	0.06
	>45	63	0.66 ± 0.23	
Functional status	Functional	33	0.76 ± 0.43	0.13
	Nonfunctional	49	0.93 ± 0.45	
Macro		74	0.62 ± 0.20	0.03
Micro		8	0.04 ± 0.02	
Hardy's grading	A, B	33	0.28 ± 0.06	0.2
	C, D, E	41	0.89 ± 0.35	
Invasive		23	1.35 ± 0.61	0.005
Noninvasive		50	0.25 ± 0.06	
Progression	<5 %	4	0.13 ± 0.08	0.08
(volume/mo)	≥5 %	7	0.83 ± 0.31	

only in the iNOS IR between invasive adenomas and noninvasive adenomas ($P < 0.05$) (Table 3). The iNOS IR had a significant correlation with the MIB-1 LI ($P < 0.05$) (Fig. 4).

Discussion

This study shows that all isoforms of NOS, especially iNOS IR, were significantly upregulated in relation to the invasiveness and MIB-1 LI in nonfunctioning adenomas and acromegaly cases, compared with the other types of tumors and control tissue.

Previous studies have reported that invasive and larger pituitary adenomas [10], or recurrent nonfunctioning adenomas with rapid progression have a high MIB-1 LI [11], while other studies have shown that the invasiveness and tumor size have no relationship with the MIB-1 LI [12]. Our present results showed that the larger and more invasive nonfunctioning adenomas and prolactinomas were associated with a higher MIB-1 LI. There was no significant difference with regard to the relationship between the MIB-1 LI and tumor progression. These results may be due to the small number of cases. On the other hand, there have been some reports about NOS expression in human pituitary adenomas [1, 7–9]. For example, nNOS was shown to be upregulated in both pituitary adenomas and in the normal pituitary gland, especially in pituitary adenomas, and iNOS is mildly upregulated in both types of tissues [1]. eNOS is upregulated in both adenoma cells and endothelial cells [8], or in only endothelial cells [1]. Our study also showed the same results as above. eNOS was also upregulated in both adenoma cells and endothelial cells, although the number of cases was modest.

The clinical significance of NOS expression in pituitary adenomas is still unclear, although there have been some

Table 3 Comparison between nitric oxide synthase IR and clinical variables

Variable	Variable groups	nNOS IR			Chi square	iNOS IR			Chi square	eNOS IR			Chi square	eNOS IR(v)			Chi square
		0	≥1			0	≥1			0	≥1			0	≥1		
Age(y)	≤45	17	3	20	0.54	16	4	20	0.02	17	3	20	1	19	0	19	0.57
	>45	48	14	62		29	32	61		53	9	62		55	4	59	
Functional status	Functional	25	7	32	0.88	18	13	31	0.72	27	5	32	0.9	28	2	30	0.64
	Nonfunctional	41	9	50		27	23	50		43	7	50		46	2	48	
Macro		60	14	74	0.35	41	32	73	0.97	63	11	74	1	66	4	70	1
Micro		5	3	8		4	4	8		7	1	8		8	0	8	
Hardy's grading	A, B	25	8	33	0.45	17	15	32	0.64	26	7	33	0.29	29	1	30	0.63
	C, D, E	35	6	41		24	17	41		37	4	41		37	3	40	
Invasive		19	4	23	0.2	6	16	22	0.004	21	2	23	0.49	21	1	22	1
Noninvasive		46	3	49		39	20	59		49	10	59		53	3	56	
Progression	<5 %	4	0	4	0.49	2	2	4	0.58	4	0	4	1	4	0	4	1
(volume/mo)	≥5 %	5	2	7		2	5	7		6	1	7		7	0	7	

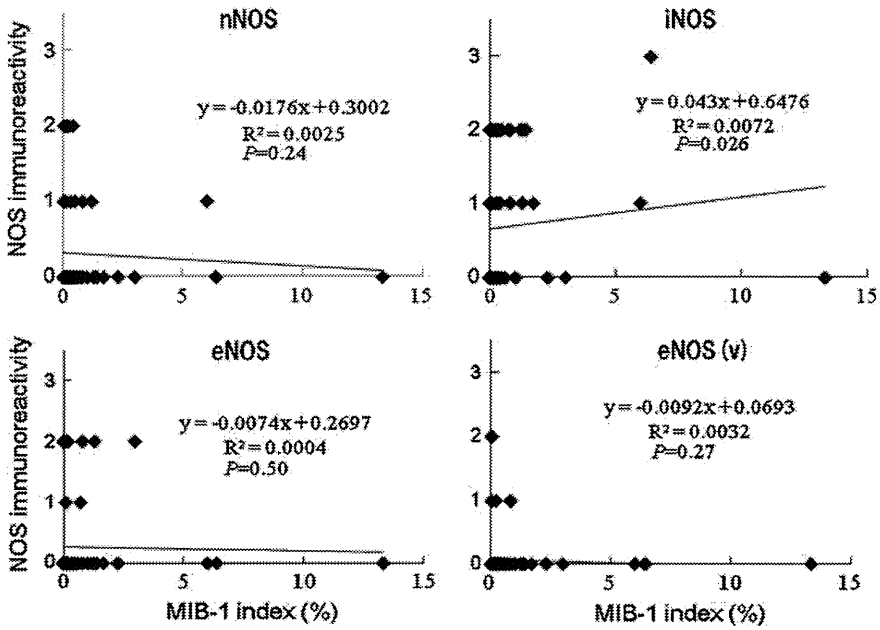

Fig. 4 The correlation between the MIB-1 labeling index and NOS immunoreactivity. *Inset*, the linear regression equation, R2 and *P* from the Spearman correlation test

studies that have speculated that NOS may regulate the blood flow and endocrine activity in adenomas [7].

Our study did not suggest any role of NOS in the endocrine activity, because no relationship was found between NOS expression and functional and nonfunctional adenomas. However, there was a relationship between iNOS expression and the invasiveness of adenomas. iNOS, which originates from macrophages, plays an important role in tissue injury and repair. Some reports have shown that iNOS has a relationship with the growth and invasiveness of other tumors [13]. Therefore, iNOS may be upregulated in adenomas with high invasiveness, as was noted in our results. There was a significant correlation between the MIB-1 LI and iNOS IR in the present study, further supporting a potential role for iNOS in adenomas.

Half of our cases with upregulated eNOS showed hemorrhage or a cyst after hemorrhage in the preoperative MRI. The upregulation of eNOS in these hemorrhagic adenomas may have been due to the fact that eNOS contributes to regulating the blood flow.

Future studies are needed to further analyze the expression of the NOS isoforms in adenomas by quantitative assessments, such as in situ hybridization.

Acknowledgments This work was supported by Grant-in Aid for Scientific Research (C) (#25350534) from the Ministry of Education, Culture, Sports, Science, and Technology, Japan. We thank Dr. Shigeo Yokoyama (Department of Pathology, Oita University Faculty of Medicine, Oita, Japan) and Dr. Kashima Kenji (Department of Pathology, Oita University Faculty of Medicine, Oita, Japan) for donating the tissue specimens from a patient with pituitary adenoma and from the autopsy cases.

Conflict of interest None.

References

1. A. Kruse, H. Broholm, I. Rubin, K. Schmidt, M. Lauritzen, Nitric oxide synthase activity in human pituitary adenomas. Acta Neurol. Scand. **106**, 361–366 (2002)
2. R.F. Furchgott, J.V. Zawadzki, The obligatory role of endothelial cells in the relaxation of arterial smooth muscle by acetylcholine. Nature **288**, 373–376 (1980)
3. S. Moncada, The L-arginine: nitric oxide pathway. Acta Physiol. Scand. **145**, 201–227 (1992)
4. R.M.J. Palner, D.S. Ashton, S. Moncada, Vascular endothelial cells synthesize nitric oxide from L-arginine. Nature **333**, 664–666 (1988)
5. Radomski MW, Moncada S, Biological role of nitric oxide in platelet function. Madrid: EDICOMPLET 45–56 (1991)
6. H. Togashi, I. Sakuma, M. Yoshioka, A central nervous system action of nitric oxide in blood pressure regulation. J. Pharmacol. Exp. Ther. **262**, 343–347 (1992)
7. T. Rubinek, H. Rubinfeld, M. Hadani, G. Barkai, I. Shimon, Nitric oxide stimulates growth hormone secretion from human fetal pituitaries and cultured pituitary adenomas. Endocrine **28**, 209–216 (2005)
8. R.V. Lloyd, L. Jin, X. Qian, Nitric oxide synthase in the human pituitary gland. Am. J. Pathol. **146**, 86–94 (1995)
9. M. Pawlikowski, K. Winczyk, M. Jaranowska, Immunohistochemical demonstration of nitric oxide synthase (NOS) in the normal rat pituitary gland, estrogen-induced rat pituitary tumor and human pituitary adenomas. Folia Histochem. Cytobiol. **41**, 87–90 (2003)
10. C. Geeta, G.C. Ari, K. Kalman, W.S. Brend, M. Sunithi, J.P. Muliyil, M.S. Seshadri, The clinical significance of MIB-1 labeling index in pituitary adenomas. Pituitary **13**, 337–344 (2010)

11. W.N. Tae, J.J. Hyeong, K.L. Mi, S.K. Tai, H.K. Sun, J.L. Eun, Predicting recurrence of nonfunctioning pituitary adenomas. J. Clin. Endocrinol. Metab. **94**, 4406–4413 (2009)
12. G. Roger, S. Brooke, H.W. Tessa, Role of Ki-67 proliferation index and p53 expression in prediction progression of pituitary adenomas. Hum. Pathol. **39**, 758–766 (2008)
13. V. Kostourou, J.E. Cartwright, A.P. Johnstone, J.K. Boult, E.R. Cullis, G. Whitley, S.P. Robinson, The role of tumour-derived iNOS in tumour progression and angiogenesis. Br. J. Cancer **104**, 83–90 (2011)

Neuro-Oncology Advance Access published November 26, 2013

Neuro-Oncology

Neuro-Oncology 2013; **0**, 1–7, doi:10.1093/neuonc/not144

H3F3A K27M mutations in thalamic gliomas from young adult patients

Koki Aihara, Akitake Mukasa, Kengo Gotoh, Kuniaki Saito, Genta Nagae, Shingo Tsuji, Kenji Tatuno, Shogo Yamamoto, Shunsaku Takayanagi*, Yoshitaka Narita, Soichiro Shibui, Hiroyuki Aburatani and Nobuhito Saito

Department of Neurosurgery, Graduate School and Faculty of Medicine, The University of Tokyo, Tokyo, Japan (K.A., A.M., K.S., S.T., N.S.); Genome Science Division, Research Center for Advanced Science and Technology, The University of Tokyo, Tokyo, Japan (K.A., K.G., G.N., S.T., K.T., S.Y., H.A.); Department of Neurosurgery and Neuro-Oncology, National Cancer Center Hospital, Tokyo, Japan (Y.N., S.S.)*

Corresponding authors: Akitake Mukasa, MD, PhD, Department of Neurosurgery, The University of Tokyo Hospital, 7-3-1 Hongo, Bunkyo-ku, Tokyo 113-8655, Japan (mukasa-nsu@umin.ac.jp); Hiroyuki Aburatani, MD, PhD, Genome Science Division, Research Center for Advanced Science and Technology (RCAST), The University of Tokyo, 4-6-1 Komaba, Meguro-ku, Tokyo 153-8904, Japan (haburata-tky@umin.ac.jp).

Introduction: Mutations in *H3F3A*, which encodes histone H3.3, commonly occur in pediatric glioblastoma. Additionally, *H3F3A* K27M substitutions occur in gliomas that arise at midline locations (eg, pons, thalamus, spine); moreover, this substitution occurs mainly in tumors in children and adolescents. Here, we sought to determine the association between *H3F3A* mutations and adult thalamic glioma.

Methods: Genomic *H3F3A* was sequenced from 20 separate thalamic gliomas. Additionally, for 14 of the 20 gliomas, 639 genes—including cancer-related genes and chromatin-modifier genes—were sequenced, and the Infinium HumanMethylation450K BeadChip was used to examine DNA methylation across the genome.

Results: Of the 20 tumors, 18 were high-grade thalamic gliomas, and of these 18, 11 were from patients under 50 years of age (median age, 38 y; range, 17–46), and 7 were from patients over 50 years of age. The *H3F3A* K27M mutation was present in 10 of the 11 (91%) younger patients and absent from all 7 older patients. Additionally, *H3F3A* K27M was not detected in the 2 diffuse astrocytomas. Further sequencing revealed recurrent mutations in *TP53*, *ATRX*, *NF1*, and *EGFR*. Gliomas with *H3F3A* K27M from pediatric or young adult patients had similar, characteristic DNA methylation profiles. In contrast, thalamic gliomas with wild-type *H3F3A* had DNA methylation profiles similar to those of hemispheric glioblastomas.

Conclusion: We found that high-grade thalamic gliomas from young adults, like those from children and adolescents, frequently had *H3F3A* K27M.

Keywords: thalamic glioma, young adult, *H3F3A* mutation.

Gliomas of the thalamic region are relatively rare and constitute ~1% of all brain tumors.[1–3] Thalamic gliomas are generally difficult to treat because the tumors are located deep within the brain and, therefore, are rarely amenable to radical surgical resection.[4] Thus, development of a novel anticancer drug is needed to treat these tumors. Schwartzentruber et al[5] recently reported that more than 30% of pediatric glioblastoma multiforme (GBM) tumors carry a mutation in the *H3F3A* gene, which encodes the replication-independent histone 3 variant H3.3. There are 2 common mutations (K27M and G34R/V) in human *H3F3A* that each result in an amino acid substitution within the histone tail. In a study of 784 glioma samples of all grades and histological diagnoses and from patients of all ages, the *H3F3A* K27M mutation was highly specific to GBM and was found mainly in younger patients (median age, 11 y; range, 5–29), including several patients with thalamic GBM. Wu et al[6] also reported a high frequency of *H3F3A* mutations in pediatric gliomas and that 78% of diffuse intrinsic pontine gliomas (DIPGs) and 22% of nonbrainstem pediatric GBM carry a mutation in *H3F3A* or in a related gene, *HIST1H3B*, which encodes the histone H3.1; each of these mutations causes a K27M amino acid substitution in the respective protein. Sturm et al[7] further showed that these mutant tumors have distinct methylation profiles and that the *H3F3A* K27M mutation most often occurs in tumors located in the midline of the brain, such as in the thalamus, brainstem, or spine. In contrast, G34R/V mutations were found in hemispheric gliomas. Although 71%–78% of DIPGs are known to have a K27M mutation,[6,8] to our knowledge no study has focused on the *H3F3A* K27M mutation in thalamic gliomas. Here, we analyzed the prevalence and significance of the K27M mutation, especially for adult patients with thalamic glioma.

Received 16 May 2013; accepted 4 August 2013

Materials and Methods

Patients and Samples

From April 1997 to March 2013, 27 adult patients (>16 y of age) with primary thalamic glioma were treated at Tokyo University Hospital or the National Cancer Center Hospital (Table 1). Histological diagnoses were made by a senior neuropathologist from the respective treatment centers and according to World Health Organization guidelines. There were 15 GBM, 9 anaplastic astrocytomas (AAs), and 3 diffuse astrocytomas (DAs). Of the 3 low-grade gliomas, 2 were located bilaterally; in contrast, most high-grade gliomas were not bilateral (left, 12; right, 11; bilateral, 1). We were able to obtain samples of freshly frozen tumor tissue for 16 of the 27 cases; and for 14 of these 16 cases, paired, normal blood samples were available; moreover, formalin-fixed, paraffin-embedded samples of tumor tissue were available for 4 of the other 11 cases. In all, tissue samples were available for 20 of the 27 cases. The study was approved by the ethics committees of the University of Tokyo Hospital and the National Cancer Center Hospital. Each patient provided written informed consent.

DNA Extraction

The AllPrep DNA/RNA Micro kit (Qiagen) was used according to the manufacturer's instructions to extract genomic DNA from freshly frozen tumor tissue. Formalin-fixed, paraffin-embedded samples were deparaffinized with xylene, and a QIAamp DNA Mini kit (Qiagen) was then used to extract genomic DNA from these tumor samples. For the 14 cases for which tumor tissues and a paired, normal blood sample were available, a DNA extraction kit (Qiagen) was used to extract control genomic DNA from the paired blood sample.

Sanger Sequencing

For the 20 cases in which DNA from tumor tissue was available, the Sanger method was used to sequence the DNA. Oligo primers were designed to amplify a target region within *H3F3A* (sense 5′- TCAATGCTGGTAGGTAAG TAAGGA -3′, antisense 5′- GGTTTCTTCACCCCTCCAGT -3′; product size: 152 bp). The high-fidelity DNA polymerase KOD-plus (Toyobo) and optimized thermal conditions were used to perform PCR, and the PCR products

Table 1. Patient characteristics and *H3F3A* status

Sample ID	Age	Location	OS (mo)	Surgery	Treatment	*H3F3A*	*MGMT* Promoter
GBM1[a,b]	17	Right	8.9	PR	RT + TMZ	K27M	u
AA1	19	Bilateral	30.6	Biopsy	RT + ACNU	-	-
AA2[a,b]	20	Left	9.9	Biopsy	RT + TMZ	K27M	u
GBM2[a,b]	27	Multiple[d]	3.8	PR	RT + TMZ	K27M	u
GBM3[a,b]	34	Right	12.6	STR	RT + ACNU	K27M	u
AA3	37	Right	26.1	Biopsy	RT + TMZ	K27M	-
GBM4[a,b]	38	Left	9.8	Biopsy	RT + TMZ	K27M	u
AA4	38	Left	17.7	Biopsy	RT + ACNU	WT	-
GBM5[a,b]	39	Right	10.4	PR	RT + TMZ	K27M	u
AA5[b]	41	Left	20.6	PR	RT + TMZ	K27M	u
AA6[a,b]	43	Left	15.6	Biopsy	RT + TMZ	K27M	m
GBM6	45	Left	30.8	Biopsy	RT + ACNU	-	-
GBM7[a,b]	46	Right	1.6[f]	GTR	RT + TMZ	K27M	u
AA7	47	Right	24.3	Biopsy	RT + ACNU	-	-
GBM8	48	Left	65.8	Biopsy	RT + TMZ	-	-
GBM9[b]	50	Right	3.9	Biopsy	RT + TMZ	WT	u
GBM10	53	Left	7.3	Biopsy	RT + TMZ	-	-
AA8[a,b,c]	57	Multiple[e]	110.2[f]	Biopsy	RT + ACNU	WT	m
GBM11[a,b,c]	62	Left	19.4	Biopsy	RT + TMZ	WT	u
GBM12[a,b]	64	Left	30.4	STR	RT + TMZ	WT	m
GBM13[a]	71	Left	3.5	Biopsy	RT + TMZ	WT	-
GBM14	73	Left	17.9	Biopsy	RT + TMZ	-	-
GBM15[a,b]	73	Right	0.7	Biopsy	RT + TMZ	WT	u
AA9	78	Right	0.3	Biopsy	No therapy	WT	-
DA1	28	Bilateral	21.1	Biopsy		-	-
DA2[a]	29	Bilateral	9.2[f]	Biopsy		WT	-
DA3	30	Left	124.4[f]	Biopsy		WT	-

Abbreviations: OS, overall survival; GTR, gross total resection; STR, subtotal resection; PR, partial resection; RT, radiotherapy; TMZ, temozolomide; ACNU, nimustine hydrochloride; WT, wild-type; m, methylated; u, unmethylated; -, not available.
[a]Specimen subjected to targeted sequence analysis.
[b]Specimen subjected to global methylation profile analysis.
[c]Specimen of recurrence.
[d]Right thalamus, left temporal lobe, and fourth ventricle.
[e]Right thalamus, left cerebellopontine angle, cerebellum surface, and fourth ventricle.
[f]Still alive at last follow-up.

were then evaluated on a 2% agarose gel and subsequently purified. The Big Dye Terminator kit (Applied Biosystems) was used for each sequencing reaction; both strands of each PCR product were sequenced, and each sample was analyzed on an ABI 3130xl capillary sequencer (Applied Biosystems).

Targeted Sequencing

For the 14 cases for which a tumor sample and a paired, normal blood sample were available, we used the Haloplex system (Agilent) to amplify and analyze the sequences of 639 selected genes (see Supplementary Table S1). These selected genes included *H3F3A, HIST1H3B*, genes often mutated in gliomas (such as *IDH1/2, ATRX, TP53, NF1, EGFR, PDGFRA*), other frequently mutated cancer genes, and chromatin-modifier genes. Target regions were enriched using Haloplex technology following the manufacturer's protocols. A Hiseq2500 system (Illumina) set in rapid mode was used to sequence the amplified targets as 150-bp paired-end reads. The median coverage was 348-fold, and more than 93% of target regions were covered by at least 10 reads (see Supplementary Table S2). The Burrows-Wheeler Aligner algorithm v0.5.9[9] was used to map this sequence data onto the reference genome (hg19), and somatic mutations were identified with the Genome Analysis Toolkit Unified Genotyper v1.6.13.[10] The tumor-specific mutations were identified by comparing results from tumor DNA and blood DNA and were annotated with Annovar (23 October 2012).[11] Finally, we used the Integrative Genomics Viewer v2.2[12] to check these mutations, and we excluded artifact mutations.

Methylation-specific PCR

The EZ DNA Methylation kit (Zymo Research) was used according to the manufacturer's protocol to conduct bisulfite reactions with each genomic DNA sample (250 ng). DNA methylation status of the O^6-methylguanine methyltransferase (*MGMT*) promoter was then determined by methylation-specific PCR as described by Esteller et al.[13]

Global Analysis of DNA Methylation

The Infinium HumanMethylation450 BeadChip (Illumina) was used according to the manufacturer's instructions to examine the genome-wide DNA methylation profiles of 14 high-grade thalamic gliomas. Previously published[7] methylation data from additional glioblastoma samples ($n = 136$) and from control samples ($n = 6$; 2 adult normal brain and 4 fetal normal brain) were obtained from the National Center for Biotechnology Information's Gene Expression Omnibus (http://www.ncbi.nlm.nih.gov/geo). The following filtering steps were used to select probes for unsupervised clustering analysis. Probes targeting the X and Y chromosomes and probes containing a single nucleotide polymorphism (dbSNP130 common) within 5 base pairs of and including the targeted cytosine-phosphate-guanine (CpG) site were removed. The standard deviation of β-values for each probe was calculated, and the top 8000 probes were selected.

Statistical Analysis

Overall survival was analyzed using the Cox regression analysis or the Kaplan-Meier method, and the log-rank test was used to make universal assessments of Kaplan-Meier plots. The frequency of methylation of the *MGMT* promoter and of other genes was analyzed by Fisher's exact test, and Welch's *t*-test was used to compare the average age of the *H3F3A* K27M group with that of the wild-type *H3F3A* group. $P < .05$ was considered significant. Statistical calculations were carried out using R v2.15.2 (http://www.cran.r-project.org).

Results

Frequency and Characteristics of Patients Harboring the H3F3A *K27M* Mutation

Among the 18 high-grade thalamic gliomas that we subjected to sequence analysis, 10 (56%) tumors had an *H3F3A* K27M mutation, while none of the 18 tumors harbored an *H3F3A* mutation at G34. Remarkably, 10 (91%) of the 11 tumors that were from patients under 50 years of age (median age, 38 y; range, 17-46) had the *H3F3A* K27M mutation; in contrast, the *H3F3A* K27M mutation was not found in any of the 7 tumors that were from patients over 50 years of age (Table 1). The patients with the *H3F3A* K27M mutation were significantly younger than those with wild-type *H3F3A* alleles (34.2 vs 61.6 y; $P = .0003$). The *H3F3A* K27M mutation was not detected in DAs from patients who were 29 or 30 years of age.

Targeted Sequence Analyses for Selected Genes

Among the 14 cases that were subject to targeted sequence analysis, tumor DNA samples from cases GBM4 and GBM11 each had mutations in mismatch repair genes and had a higher than average number of mutations; the average number of nonsynonymous mutations in DNA samples from all tumors except these 2 GBM specimens was 3.83 (0-8) (see Supplementary Table S3), while the numbers of nonsynonymous mutations in the DNA samples from GBM4 and GBM11 were 32 and 165, respectively. GBM4 had a mutation in the mismatch repair gene *MSH2* (MutS homolog 2). In the case of GBM11, which recurred after treatment with the alkylating agent temozolomide, mutations were identified in 2 mismatch repair genes, *PMS2* (postmeiotic segregation increased 2) and *MLH3* (MutL homolog 3); moreover, 158 (96%) of 165 mutations found in this tumor were G/C to A/T transitions. Therefore, GBM11 apparently had a hypermutator phenotype.[14] Because most of the mutations in these 2 cases (GBM4 and GBM11) could have accumulated passively owing to the lack of mismatch repair function, we excluded the mutation data from these cases from the subsequent analyses.

Consistent with previously reported data,[5] *H3F3A*-mutant high-grade gliomas frequently also had mutations in *TP53, ATRX* (2/7 [28.6%] of *H3F3A* K27M-mutant tumors vs 0/4 [0%] of wild-type *H3F3A* tumors; $P = .49$), and *NF1* (3/7 [42.9%] vs 0/4 [0%]; $P = .24$) (Fig. 1). In contrast, wild-type *H3F3A* tumors had *EGFR* mutations more frequently than did *H3F3A* K27M-mutant tumors (0/7 [0%] vs 2/4 [50%]; $P = .11$). There were no recurrent mutations other than *H3F3A, TP53, ATRX, NF1*, and *EGFR*. Wu et al[6] reported that 18% of DIPGs had a *HIST1H3B* K27M mutation, but we did not find *HIST1H3B* mutations in any of the 14 tissue samples evaluated, even in samples from wild-type *H3F3A* tumors. Additionally, none of the 14 tumors examined had an *IDH1* or an *IDH2* mutation.

Recently, Fontebasso et al[15] found that mutations in the *SETD2* gene, which encodes an H3K36 trimethyltransferase, occurred in 15% of hemispheric pediatric GBMs, and mutations in *SETD2* and *H3F3A* were mutually exclusive. Based on these findings, we also sequenced genes that potentially affect histone modification, such as the H3K27 methyltransferase *EZH2*, the H3K27 demethylase *KDM6A*, the H3K27 acetyltransferase *EP300*, and *CREBBP*. We identified a *KDM6A* mutation (p.R1213L), located in

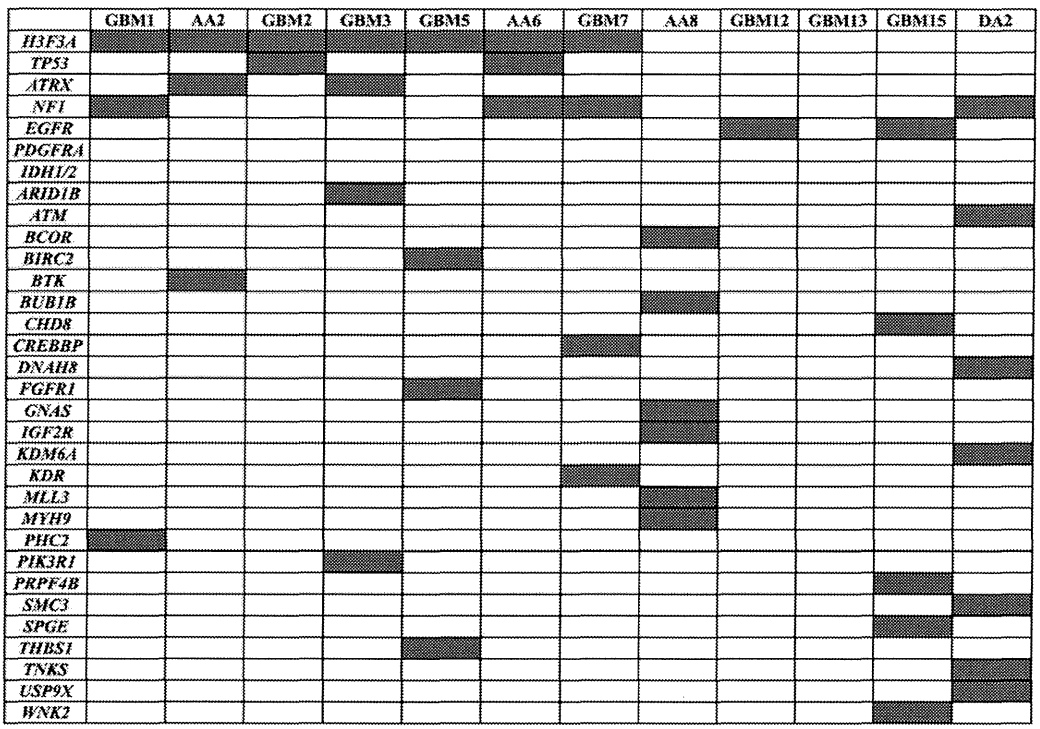

Fig. 1. Nonsynonymous mutations identified via targeted sequencing. Each row represents a specific gene, and each column represents one sample. The shaded boxes represent identified nonsynonymous mutations.

the JmjC domain, in one case of DA with wild-type *H3F3A* and a *CREBBP* mutation in one case of GBM with the *H3F3A* K27M mutation. However, we did not find mutations in any of these genes in any of the 4 analyzed cases of high-grade glioma that lacked an *H3F3A* K27M mutation.

In addition, we found an *FGFR1* mutation (N546K) in one GBM (GBM5) with *H3F3A* K27M. Schwartzentruber et al[5] also reported an *FGFR1* mutation (K656E) in an *H3F3A* K27M-mutant tumor.[3] Both of these *FGFR1* mutations reportedly enhance kinase activity.[15]

Methylation Status of the MGMT *Promoter*

We analyzed methylation at the *MGMT* promoter in samples from 14 adults with high-grade gliomas whose DNA was suitable for such analysis; the *MGMT* promoter in 11 (79%) of these tumors was unmethylated. In particular, the *MGMT* promoter was frequently unmethylated in samples of thalamic glioma with an *H3F3A* K27M mutation from young adults (8/9; 89%). The rate of unmethylated *MGMT* promoter was higher in the group of samples analyzed in this study than in a group of high-grade gliomas from all locations that we analyzed previously (43/75; 57%),[16] but the difference between these rates was not statistically significant ($P = .23$).

Global DNA Methylation Profiles of Thalamic Gliomas

The genome-wide Infinium methylation data demonstrated that adult thalamic high-grade gliomas with the *H3F3A* K27M mutation had methylation profiles distinct from those of adult thalamic high-grade gliomas that lacked the *H3F3A* K27M mutation (Fig. 2). In the hierarchal clustering analysis that included methylation profile data from previously categorized pediatric and adult gliomas,[7] the adult thalamic high-grade gliomas harboring the *H3F3A* K27M mutation clustered within the same "K27" category as did the pediatric gliomas harboring *H3F3A* K27M. In contrast, adult thalamic high-grade gliomas with wild-type *H3F3A*, which had a variety of methylation profiles, did not cluster into the K27 category, but clustered within several other categories, including "mesenchymal" and "classic." One recurrent anaplastic astrocytoma (AA8) that was wild-type for *H3F3A* had a profile that was similar to those of the tumors in the K27 category, but this profile seemed to be located outside the cluster in the K27 category.

Prognostic Value of the H3F3A *K27M Mutation*

For the 16 cases for which a primary tumor sample was analyzed, the median overall survival of patients with GBM and those with AA was 8.9 months and 15.6 months, respectively. The median overall survival of patients with high-grade gliomas (GBM or AA) was 9.9 months, and progression-free survival of these patients was 5.3 months. In these cases of high-grade glioma, the median overall survival of patients with *H3F3A* K27M-mutant tumors was 10.4 months (GBM, 9.8 mo; AA, 15.6 mo) and that of patients with wild-type *H3F3A* tumors was 3.5 months (GBM, 3.5 mo; AA, 0.3 mo). There was no statistical difference in overall survival ($P = .80$) or progression-free survival (6.0 vs 1.8; $P = .44$) between these 2 groups (Fig. 3).

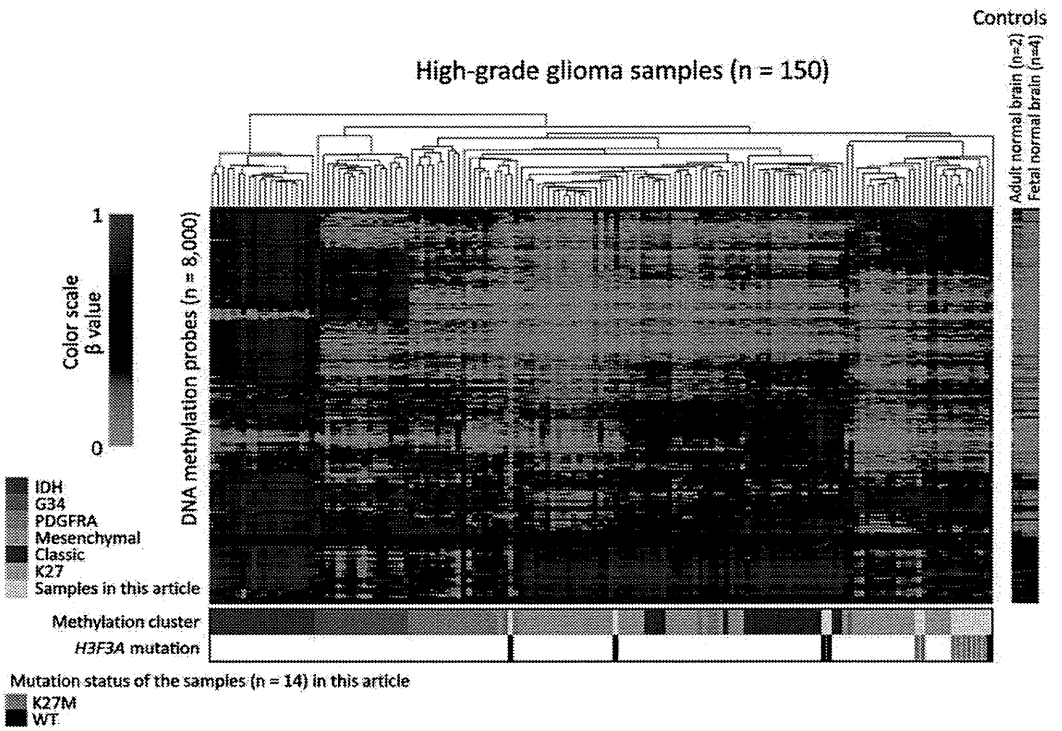

Fig. 2. Heatmap of methylation levels (β-value) in 150 high-grade gliomas, including 14 thalamic gliomas analyzed in this study. Supervised clustering was performed using 8000 selected Infinium probes. Each row represents a probe, each column represents one sample. For each sample, annotation of methylation cluster and *H3F3A* mutation status are indicated by colored boxes at the bottom of the map.

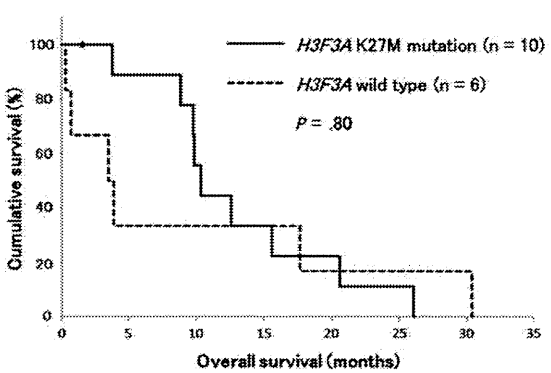

Fig. 3. Kaplan–Meier estimates of overall survival in cases of high-grade thalamic gliomas. There was no statistical difference in overall survival between patients with *H3F3A* K27M-mutant tumors and those with wild-type *H3F3A* tumors.

The Cox regression analysis assessing 3 variables—*H3F3A* K27M mutation status, *MGMT* methylation, and age—showed no significant difference in overall survival due to any one variable (*H3F3A* mutation: hazard ratio [HR] = 0.11, 95% confidence interval [CI] = 0.0057–2.2, $P = .15$; *MGMT* methylation: HR = 0.088, 95% CI = 0.0054–1.4, $P = .088$; and age: HR = 0.96, 95% CI = 0.88–1.1, $P = .38$).

Discussion

Here, we showed that the *H3F3A* K27M mutation was common in high-grade thalamic gliomas in young adults, as is the case for GBM in children and adolescents.[17] Reportedly, 80% of pediatric thalamic GBM tumors harbor the *H3F3A* K27M substitution,[5,7,17] as do 71%–78% of DIPGs;[6,8] however, the occurrence of this substitution in adult thalamic glioma has not been examined. We found that the *H3F3A* K27M mutation was highly prevalent in cases of thalamic GBM in young adults; moreover, this mutation was found in 90% (9/10 cases) of high-grade thalamic gliomas in patients between 20 and 46 years of age. In contrast to *IDH* mutations, the *H3F3A* K27M mutation seemed infrequent in low-grade gliomas; DAs from patients of 29 or 30 years of age did not have the *H3F3A* K27M mutation. For DIPGs, a small number of low-grade astrocytomas were reported to have the *H3F3A* K27M mutation,[8] but in general the *H3F3A* K27M mutation seemed to be specific to high-grade gliomas.[5,7,18]

H3F3A encodes H3.3, a specialized histone variant. H3.3 is deposited on chromatin in a replication-independent manner and is enriched at actively transcribed genes and heterochromatic regions, such as telomeres and pericentromeric regions.[19] Histone 3 lysine 27 trimethylation (H3K27me3), which is mediated by the histone-methyltransferase enhancer of zeste homolog 2 (EZH2), a member of the Polycomb family, is associated with the silencing of transcription.[20] Reportedly, tumors with the *H3F3A* K27M

mutation have little or no H3K27me3, and they have increased acetylation of H3K27 (H3K27ac); conversely, tumors with wild-type *H3F3A* have increased H3K27me3 and lowered H3K27ac levels.[21,22] Although the mutated histone variant H3.3 accounts for only a small proportion of the entire histone H3 population, reduction of H3K27me3 occurs globally and affects other histone H3 molecules because the K27M peptide reduces the methyltransferase activity of Polycomb repressive complex 2 (PRC2) by inhibiting the catalytic subunit EZH2, which contains a Su(var)3-9/enhancer-of-zeste/trithorax (SET) domain.[22] Moreover, inhibition of PRC2 leads to increased levels of H3K27 acetylation, which is a marker of active enhancers.[23] In fact, gliomas with the *H3F3A* K27M mutation were shown to form a class with a distinctive methylation profile of CpG islands that probably resulted from epigenetic dysregulation.[7] However, the mechanisms by which this dysregulation of histone modification leads to gliomagenesis is unknown. We reasoned that the thalamic gliomas lacking the *H3F3A* mutation might result from a similar mechanism of tumorigenesis as tumors harboring the *H3F3A* K27M mutation; therefore, we performed targeted gene sequencing of molecules that could modulate H3K27 status. The targeted genes included *EZH2*, *KDM6A*, *EP300*, and *CREBBP*. We identified a *KDM6A* mutation (p.R1213L) in one case of DA. This mutation was located in the JmjC domain, and might have similar tumorigenic potential as the *H3F3A* K27M mutation. We also identified a *CREBBP* mutation in a tumor with the *H3F3A* K27M mutation; however, we did not find mutations in any of these genes in the high-grade tumors that lacked the *H3F3A* K27M mutation. Therefore, high-grade thalamic gliomas with wild-type *H3F3A* might have resulted from a tumorigenic mechanism that is not related to H3.3 K27 modifications. However, we did not identify any other driver mutation. Genomic analysis on a larger scale might be required to reveal novel mutations, but thalamic gliomas are rare and biopsy is the standard surgical procedure; therefore, such a large-scale analysis of these gliomas will be difficult.

To further evaluate the molecular characteristics of *H3F3A* K27M-mutant thalamic gliomas, global methylation profiles were examined; the adult thalamic high-grade gliomas with the *H3F3A* K27M mutation had methylation profiles similar to those of *H3F3A* K27M-mutant pediatric glioblastomas. This finding indicated that patient age did not affect the pattern of methylation in K27M-mutant tumors. In contrast, *H3F3A* wild-type adult thalamic high-grade gliomas, which occurred mostly in patients over 50 years of age, shared the molecular characteristics with hemispheric glioblastomas; this finding was expected based on the fact that molecules that could modulate H3K27 status were not mutant in these tumors. These results raised the possibility that treatment strategies in cases of adult glioblastomas should be designed based on tumor location and *H3F3A* mutation status.

In this set of cases, the median overall survivals were only 8.9 months and 15.6 months for patients with GBM and those with AA, respectively. These periods of survival were shorter than the average overall survival among patients with GBM or AA.[24] These gliomas, because of their location, were not amenable to radical tumor resection, and this characteristic might be one reason for the poor outcomes, as the degree of surgical resection is an important prognostic factor.[25] Indeed, diagnostic biopsy was the sole surgical intervention in most of these cases. The absence of *IDH1* and *IDH2* mutations, which were found in ~30% of AA and 10% of GBM in our previous report[16] and are good prognostic markers of longer survival, might also account for the poor prognosis of patients with thalamic gliomas. We also suspected that the low frequency of methylated *MGMT* promoters, which are the key indicators of poor response to temozolomide and are among the most important prognostic factors,[26] might explain the poor survival among younger patients with thalamic glioma who underwent intensive chemoradiotherapy. Indeed, the patients with methylated *MGMT* promoters lived longer than those with unmethylated *MGMT* promoters, but this difference was not statistically significant. In addition, we suspected that *H3F3A* K27M mutation in thalamic gliomas might be associated with poor survival, because *H3F3A* K27M-mutant DIPGs were reportedly associated with worse overall survival than were wild-type tumors.[8] However, in this study, there was no significant difference in overall survival between patients with *H3F3A* K27M-mutant gliomas, which occurred mostly in younger patients, and those with wild-type *H3F3A* gliomas, which occurred mostly in older patients. Nevertheless, our sample size was small, and the prognostic significance of *H3F3A* K27M mutation for thalamic gliomas must be examined further in larger studies.

In conclusion, thalamic gliomas in young adults, as well as those in children and adolescents, often harbor the *H3F3A* K27M mutation. Thalamic high-grade gliomas in young adults may as a group share a particular mechanism of tumorigenesis that is related to the *H3F3A* K27M mutation; therefore, development of customized treatment strategies may be required for this patient population.

Supplementary Material

Supplementary material is available online at Neuro-Oncology (http://neuro-oncology.oxfordjournals.org/).

Funding

This work was supported in part by the National Cancer Center Research and Development Fund (23-A-20), and by Grants-in-Aid for Scientific Research (B) (no. 23390343 to A.M.), Grant-in-Aid for Scientific Research (S) (no. 24221011 to H.A.), Grant-in-Aid for Scientific Research on Innovative Areas (no. 23134501 to A.M.), Grant-in-Aid for Young Scientists (B) (no. 24791486 to K.S.), and a research program of the Project for Development of Innovative Research on Cancer Therapeutics (P-Direct) (A.M., G.N., Y.N., H.A., N.S.) from the Ministry of Education, Culture, Sports, Science, and Technology of Japan. A.M. was also supported by the Takeda Science Foundation and Japan Brain Foundation.

Acknowledgments

The authors thank Reiko Matsuura and Yuko Matsushita for extracting DNA from formalin-fixed, paraffin-embedded samples and blood, Hiroko Meguro for performing the Infinium methylation assays, Kaori Shiina and Saori Kawanabe for gene sequencing, and Ruriko Miyahara for assisting with the analysis of patient information.

Conflict of interest statement. None declared.

References

1. Cheek WR, Taveras JM. Thalamic tumors. *J Neurosurg.* 1966;24(2):505–513.

2. McKissock W, Paine KW. Primary tumours of the thalamus. *Brain*. 1958; 81(1):41–63.
3. Tovi D, Schisano G, Liljeqvist B. Primary tumors of the region of the thalamus. *J Neurosurg*. 1961;18:730–740.
4. Kelly PJ. Stereotactic biopsy and resection of thalamic astrocytomas. *Neurosurgery*. 1989;25(2):185–194.
5. Schwartzentruber J, Korshunov A, Liu XY, et al. Driver mutations in histone H3.3 and chromatin remodelling genes in paediatric glioblastoma. *Nature*. 2012;482(7384):226–231.
6. Wu G, Broniscer A, McEachron TA, et al. Somatic histone H3 alterations in pediatric diffuse intrinsic pontine gliomas and non-brainstem glioblastomas. *Nat Genet*. 2012;44(3):251–253.
7. Sturm D, Witt H, Hovestadt V, et al. Hotspot mutations in *H3F3A* and *IDH1* define distinct epigenetic and biological subgroups of glioblastoma. *Cancer Cell*. 2012;22(4):425–437.
8. Khuong-Quang DA, Buczkowicz P, Rakopoulos P, et al. K27M mutation in histone H3.3 defines clinically and biologically distinct subgroups of pediatric diffuse intrinsic pontine gliomas. *Acta Neuropathol*. 2012; 124(3):439–447.
9. Li H, Durbin R. Fast and accurate short read alignment with Burrows–Wheeler transform. *Bioinformatics*. 2009;25(14):1754–1760.
10. McKenna A, Hanna M, Banks E, et al. The Genome Analysis Toolkit: a MapReduce framework for analyzing next-generation DNA sequencing data. *Genome Res*. 2010;20(9):1297–1303.
11. Wang K, Li M, Hakonarson H. ANNOVAR: functional annotation of genetic variants from high-throughput sequencing data. *Nucleic Acids Res*. 2010;38(16):e164.
12. Robinson JT, Thorvaldsdottir H, Winckler W, et al. Integrative genomics viewer. *Nat Biotechnol*. 2011;29(1):24–26.
13. Esteller M, Sanchez-Cespedes M, Rosell R, Sidransky D, Baylin SB, Herman JG. Detection of aberrant promoter hypermethylation of tumor suppressor genes in serum DNA from non–small cell lung cancer patients. *Cancer Res*. 1999;59(1):67–70.
14. Cancer Genome Atlas Research Network. Comprehensive genomic characterization defines human glioblastoma genes and core pathways. *Nature*. 2008;455(7216):1061–1068.
15. Fontebasso AM, Schwartzentruber J, Khuong-Quang DA, et al. Mutations in *SETD2* and genes affecting histone H3K36 methylation target hemispheric high-grade gliomas. *Acta Neuropathol*. 2013; 125(5):659–669.
16. Mukasa A, Takayanagi S, Saito K, et al. Significance of *IDH* mutations varies with tumor histology, grade, and genetics in Japanese glioma patients. *Cancer Sci*. 2012;103(3):587–592.
17. Fontebasso AM, Liu XY, Sturm D, Jabado N. Chromatin remodeling defects in pediatric and young adult glioblastoma: a tale of a variant histone 3 tail. *Brain Pathol*. 2013;23(2):210–216.
18. Gielen GH, Gessi M, Hammes J, Kramm CM, Waha A, Pietsch T. *H3F3A* K27M mutation in pediatric CNS tumors: a marker for diffuse high-grade astrocytomas. *Am J Clin Pathol*. 2013;139(3):345–349.
19. Goldberg AD, Banaszynski LA, Noh KM, et al. Distinct factors control histone variant H3.3 localization at specific genomic regions. *Cell*. 2010;140(5):678–691.
20. Vastenhouw NL, Schier AF. Bivalent histone modifications in early embryogenesis. *Curr Opin Cell Biol*. 2012;24(3):374–386.
21. Venneti S, Garimella MT, Sullivan LM, et al. Evaluation of histone 3 lysine 27 trimethylation (H3K27me3) and enhancer of zest 2 (EZH2) in pediatric glial and glioneuronal tumors shows decreased H3K27me3 in *H3F3A* K27M mutant glioblastomas. *Brain Pathol*. 2013;23(5): 558–564.
22. Lewis PW, Muller MM, Koletsky MS, et al. Inhibition of PRC2 activity by a gain-of-function H3 mutation found in pediatric glioblastoma. *Science*. 2013;340(6134):857–861.
23. Zhou VW, Goren A, Bernstein BE. Charting histone modifications and the functional organization of mammalian genomes. *Nat Rev Genet*. 2011;12(1):7–18.
24. Shibui S. Report of Brian Tumor Registry of Japan (1984–2000). *Neurol Med Chir (Tokyo)*. 2009;49:1–101.
25. Sanai N, Polley MY, McDermott MW, Parsa AT, Berger MS. An extent of resection threshold for newly diagnosed glioblastomas. *J Neurosurg*. 2011;115(1):3–8.
26. Hegi ME, Diserens AC, Gorlia T, et al. *MGMT* gene silencing and benefit from temozolomide in glioblastoma. *N Engl J Med*. 2005;352(10): 997–1003.

Neurologia medico-chirurgica Advance Publication Date: November 20, 2013

ORIGINAL ARTICLE doi: 10.2176/nmc.oa2012-0441

Toxicity and Outcome of Radiotherapy with Concomitant and Adjuvant Temozolomide in Elderly Patients with Glioblastoma: A Retrospective Study

Kuniaki SAITO,[1] Akitake MUKASA,[1] Yoshitaka NARITA,[2] Yusuke TABEI,[3] Nobusada SHINOURA,[3] Soichiro SHIBUI,[2] and Nobuhito SAITO[1]

[1]*Department of Neurosurgery, The University of Tokyo Hospital, Tokyo;*
[2]*Department of Neurosurgery and Neuro-Oncology, National Cancer Center Hospital, Tokyo;*
[3]*Department of Neurosurgery, Tokyo Metropolitan Cancer and Infectious Diseases Center Komagome Hospital, Tokyo*

Abstract

Radiation therapy with concomitant and adjuvant temozolomide (TMZ) is the standard therapy for nonelderly patients with glioblastoma. However, TMZ-based chemoradiotherapy for elderly patients with glioblastoma is controversial. The aim of this study was to investigate the benefits and adverse effects of this combined therapy in elderly patients with glioblastoma. Of the 76 newly diagnosed glioblastoma patients who were treated with standard radiotherapy (60 Gy/30 fractions) and TMZ, treatment toxicity and therapeutic outcome were evaluated in 27 elderly patients (age 65 years or older) and compared with those of 49 nonelderly counterparts (age younger than 65 years). The incidence of common toxicity criteria Grade 4 adverse events during the concomitant course was higher in the elderly group than that in the nonelderly group (26% versus 8%; p = 0.046). Cognitive dysfunction was observed only in the elderly group (p = 0.042). The median overall survival (OS) and median progression-free survival in the elderly group were 15.2 months (95% confidence interval [CI]; 12.9–18.5) and 8.4 months (95% CI; 5.1–11.7), respectively. OS was significantly shorter in the elderly group than in the nonelderly group (p = 0.021). The recursive partitioning analysis score was a prognostic factor for OS. TMZ-based chemoradiotherapy was associated with an increased risk of Grade 4 adverse events in the elderly patients during concomitant use. Thus, elderly patients who undergo a concomitant course of TMZ must be closely monitored for adverse events. Treatment of glioblastoma in elderly patients must be optimized to reduce toxicity to acceptable levels and to maintain efficacy.

Key words: glioblastoma, elderly, temozolomide, toxicity

Introduction

Glioblastoma multiforme (GBM) is the most common primary brain cancer, and it occurs frequently in elderly people.[1)] The elderly population is growing in many countries; therefore, the number of GBM patients diagnosed at age ≥ 65 years is expected to continue to increase. Despite intensive treatment that could include surgical resection, irradiation, chemotherapy, or some combination of these, patients with GBM have a poor prognosis and a median overall survival (OS) of a little over a year. Moreover, elderly patients are known to have even shorter survival than their younger counterparts.[2)] Based on the findings of a phase III randomized trial, radiotherapy with concomitant and adjuvant temozolomide (TMZ) is considered the standard of care for those patients with GBM who are less than 70 years old.[3)] However, subgroup analysis of this study showed diminishing benefit with increasing age, the hazard ratio being 0.80 for the 66–71 year age group (p = 0.340)[4)]; this finding indicated that combined chemoradiotherapy with this regimen may not represent the optimal approach to treatment of GBM in elderly patients. Therefore, optimization of radiotherapy and chemotherapy for elderly patients with GBM has been an important clinical concern in recent years.

Received December 26, 2012; Accepted April 8, 2013

The decreased survival benefit of TMZ-based chemoradiotherapy in elderly patients might be attributed, in part, to the toxicity of the treatment. Based on data from several reports, elderly patients who undergo the standard 6-week course of radiotherapy with concomitant TMZ chemotherapy suffer adverse events.[5–11] However, the toxicity profile of this combined chemoradiotherapy in elderly patients has not been evaluated thoroughly, particularly in Asian populations. Furthermore, comparisons between adverse events rates in elderly patients and those in younger counterparts have generally not been studied in the setting of ordinary clinical trials. We think that more and better information about the toxicity caused by TMZ-based chemoradiotherapy in elderly patients will help to improve post-operative therapy in this population; therefore, we retrospectively reviewed cases of newly diagnosed GBM that were treated with surgery and TMZ-based chemoradiotherapy in the same institutions during the same period, and we compared the adverse events and therapeutic outcome in elderly patients with those in younger counterparts.

Methods

The authors retrospectively analyzed 76 cases of newly diagnosed GBM that were treated with standard radiotherapy of 60 Gy in 30 fractions with concomitant TMZ-based chemotherapy at the University of Tokyo Hospital, the National Cancer Center Hospital, and Komagome Metropolitan Hospital between October 2004 and April 2010. Of these 76 patients, 27 patients (aged 65 years or older at diagnosis) were classified as elderly, and 49 patients (aged less than 65 years) were classified as nonelderly. The outcome and toxicity of the therapy were compared between these two groups. Patients treated with radiotherapy alone or supportive care were excluded from the analysis. No patient was treated with TMZ alone.

For each case included in the study, radiation therapy started within 2 weeks after surgery, and a total dose of 60 Gy was delivered over 6 weeks on a once-daily schedule of 2.0 Gy per fraction. Concomitant chemotherapy consisted of 75 mg/m^2/day TMZ from the first day of radiotherapy. Adjuvant TMZ was started 4 weeks after the end of radiotherapy and was delivered for 5 days every 28 days. The TMZ dose was 150 mg/m^2 for the first cycle and was increased to 200 mg/m^2 after the second cycle. Patients were closely monitored for toxicity throughout TMZ treatment, and all adverse events were recorded and graded according to the common toxicity criteria (CTC) of the National Cancer Institute, version 4.0. Hematology, complete biochemistry, and other adverse events including disturbance of cognitive function were assessed more than once a week during the concomitant course and once per cycle during the adjuvant course. TMZ was given only if neutrophils were > 1,500/μl and platelets were > 100,000/μl; otherwise, treatment was delayed until adequate recovery. If nadir neutrophil counts < 1,000 μl, nadir platelets counts < 100,000/μl, or a CTC Grade 3 nonhematologic adverse event was observed during adjuvant course, TMZ dose was reduced from 200 mg/m^2 to 150 mg/m^2 or from 150 mg/m^2 to 100 mg/m^2 in subsequent TMZ cycle. TMZ was discontinued in case the treating physician judges to discontinue for any reasons such as disease progression, severe toxicity, patient refusal, and so on. Prophylactic sulfamethoxazole-trimethoprim for *Pneumocystis jiroveci* was given routinely.

Patients were evaluated for response using magnetic resonance imaging neuroimaging, which was performed every two cycles. Tumor progression was defined based on the Macdonald criteria; specifically, the emergence of a new lesion or an increase in tumor size by at least 25% indicated tumor progression.[12]

If a frozen tumor sample from a case was available, a QIAGEN DNA extraction kit was used to extract DNA from the tumor sample. Based on methods described by Esteller et al.,[13] methylation-specific polymerase chain reaction (PCR) following sodium bisulfite DNA modification was used to assess promoter methylation of the O6-methylguanine methyltransferase (*MGMT*) gene. The study was approved by the ethics committee of the University of Tokyo Hospital. All clinical samples were obtained with written informed consent from patients.

The Kaplan-Meier method was used to calculate OS and progression-free survival (PFS), and the log-rank test was used to evaluate differences in progression and in survival in relation to prognostic factors. Comparison of subjects by descriptive or clinical demographical variables was performed by using Fisher's exact test for discrete variables and a Student's *t*-test for continuous variables. The significance level was set at $p < 0.05$. All calculations were performed using JMP version 9 software.

Results

I. Patients' characteristics

Median follow-up periods were not significantly different between the elderly group and the nonelderly group (14.4 months versus 18.9 months; $p = 0.12$). The characteristics of the elderly patients and the nonelderly patients are summarized in Table 1. In

Table 1 Clinical characteristics of elderly and nonelderly patients

	≥ 65 (n = 27)	< 65 (n = 49)	p value
Age (mean ± SD)	71.4 ± 3.8	47.1 ± 2.8	
Sex			
Male	16 (59%)	34 (69%)	0.45
Female	11 (41%)	15 (31%)	
KPS			
< 70	8 (30%)	7 (18%)	0.37
70–100	19 (70%)	31 (82%)	
RPA class			
III		10 (20%)	< 0.0001*
IV	3 (11%)	25 (51%)	
V	21 (78%)	9 (18%)	
VI	3 (11%)	5 (10%)	
Extent of resection			
GTR	6 (22%)	12 (24%)	0.65
PR	16 (59%)	24 (49%)	
Biopsy	5 (19%)	13 (27%)	
MGMT promoter			
Methylated	8 (42%)	12 (41%)	1.0
Unmethylated	11 (58%)	17 (59%)	

*Significant value. GTR: gross total removal, KPS: Karnofsky performance status, *MGMT*: O6-methylguanine methyltransferase, PR: partial removal, RPA: recursive partitioning analysis, SD: standard deviation.

the elderly group, the mean age was 71.4 ± 3.8 years. Of the 27 elderly patients, 16 were male. The Karnofsky performance status (KPS) of the elderly group was under 70 in 8 patients (30%) and 70 or more in 19 patients (70%). According to recursive partitioning analysis (RPA),[14] significantly more patients were classified into poor prognosis group (Classes V and VI) in the elderly group than in the nonelderly group (89% versus 29%; $p < 0.0001$). Methylation-specific PCR was performed in 19 of 27 elderly patients and 29 of 49 nonelderly patients. Among patients with methylation-specific PCR assessment, promoter methylation of *MGMT* was evident in approximately 40% of the patients in both the elderly and nonelderly groups. There were no significant differences between groups as to sex, KPS, extent of resection, or *MGMT* methylation.

II. Toxicity

Adverse events of CTC Grade 3 and 4 that occurred during the concomitant course (Table 2) or the adjuvant course (Table 3) were classified as hematologic or treatment-related nonhematologic. During the concomitant course, lymphocytopenia occurred frequently in both the elderly group (26%) and the nonelderly group (53%). Thrombocytopenia was more frequent in the elderly group than in the nonelderly group ($p = 0.042$); conversely, lymphocytopenia was more common in nonelderly group

Table 2 CTC Grade 3 and 4 adverse events that occurred during the course of TMZ that was administered concomitantly with radiotherapy

	Adverse event	≥ 65 (n = 27)		< 65 (n = 49)		p value
		N	%	N	%	
Hematologic	Leukocytopenia	6 (2)	22 (7)	6 (1)	12 (2)	0.33
	Neutropenia	6 (3)	22 (11)	4	8	0.15
	Lymphocytopenia	7 (3)	26 (11)	26 (3)	53 (6)	0.03*
	Thrombocytopenia	3 (3)	11 (11)	0	0	0.042*
	Overall Grade 3/4	10	37	26	53	0.23
	Overall Grade 4	7	26	4	8	0.046*
Treatment-related nonhematologic	Constipation	0	0	1	2	1.0
	Fatigue	1	4	1	2	1.0
	Pneumonia	1	2	1	2	1.0
	Liver enzyme	3	11	2	4	0.34
	Hypoalbuminemia	1	4	0	0	0.35
	Rash	0	0	1	2	1.0
	Meningitis	1	4	0	0	0.35
	Cognitive dysfunction	3	11	0	0	0.042*
	Overall Grade 3/4	8	30	6	12	0.072

*Significant value. Figures in parentheses show the number or percentage of Grade 4 adverse events. CTC: common toxicity criteria, TMZ: temozolomide.

Table 3 CTC Grade 3 and 4 adverse events that occurred during the course of adjuvant TMZ that was administered after radiotherapy

	Adverse event	≥ 65 (n = 22)		< 65 (n = 45)		p value
		N	%	N	%	
Hematologic	Leukocytopenia	1	5	9 (2)	20 (4)	0.15
	Neutropenia	1	5	2	4	1.0
	Lymphocytopenia	6 (2)	27 (5)	18 (2)	40 (4)	0.42
	Thrombocytopenia	1	5	2 (2)	4 (4)	1.0
	Overall Grade 3/4	8	36	20	44	0.6
	Overall Grade 4	2	9	3	7	1.0
Treatment-related nonhematologic	Nausea	0	0	1	2	1.0
	Anorexia	0	0	1	2	1.0
	Fatigue	1	5	0	0	0.33
	Pneumonia	3	14	2	4	0.32
	Liver enzyme	2	9	4	9	1.0
	Rash	1	5	2	4	1.0
	DVT/PE	0	0	1	2	1.0
	Cognitive dysfunction	1	5	0	0	0.33
	Viral infection	0	0	2	4	1.0
	Overall Grade 3/4	8	36	10	22	0.25

Figures in parentheses show the number or percentage of Grade 4 adverse events. CTC: common toxicity criteria, DVT: deep vein thrombosis, PE: pulmonary embolism, TMZ: temozolomide.

(p = 0.03). Although the incidence of overall Grade 3 and 4 adverse events was similar in both groups, more patients in the elderly group suffered Grade 4 hematological adverse events than did those in the nonelderly group (26% versus 8%; p = 0.046). Total 12 Grade 4 hematologic adverse events (leukocytopenia, 2; neutropenia, 3; lymphocytopenia, 4; thrombocytopenia, 3) were observed during the concomitant course in seven elderly patients. Two of 7 (29%) elderly patients with Grade 4 hematological adverse event could not start the adjuvant TMZ course because of prolonged myelosuppression. With respect to nonhematologic toxicity, cognitive dysfunction was observed in three elderly patients during concomitant course, while it was not observed in nonelderly patients (p = 0.042).

During the adjuvant course of TMZ, 4 of 22 elderly patients (18%) and 2 of 45 nonelderly patients (4.4%) required dose reduction (p = 0.46). The frequency of overall Grade 3 and 4 adverse events was comparable between the two groups. Grade 4 adverse events occurred in 9% of the elderly group and in 7% of the nonelderly group (p = 1.0) during the adjuvant course of TMZ.

III. TMZ cycle number and interval

The number and interval of TMZ cycles are shown in Table 4. The mean number of adjuvant cycles of TMZ was 4 in the elderly and 6.3 in the nonelderly. The mean number and the interval of adjuvant cycles were not significantly different between the two groups (p = 0.066 and 0.69, respectively), while the duration between the last day of the concomitant course and the first adjuvant cycle was significantly longer in the elderly group (48.4 versus 34.5 days; p = 0.01). Reasons for discontinuation of the adjuvant course included recurrence, deterioration of performance status, severe adverse effect, and patient refusal.

Table 4 Number and interval of TMZ cycles

	≥ 65	< 65	p value
Numbers of TMZ cycle	4.0 ± 2.0	6.3 ± 1.5	0.066
Interval of TMZ cycle (days)	32.4 ± 2.5	31.8 ± 1.67	0.69
Interval between concomitant TMZ and adjuvant TMZ (days)	48.4 ± 8.8	34.5 ± 5.9	0.01*

*Significant value. Each number indicates mean ± standard deviation. TMZ: temozolomide.

IV. OS and PFS

Figure 1 shows the Kaplan-Meier analysis for OS and PFS of the patients in the elderly and nonelderly groups. The median OS was 15.2 (95%

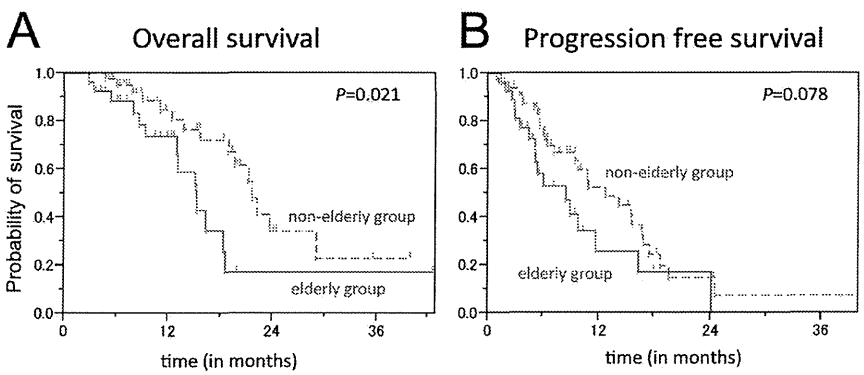

Fig. 1 Kaplan-Meier analysis for (A) overall survival and (B) progression-free survival of the patients in the elderly group and the nonelderly group.

confidence interval [CI]; 12.9–18.5) months in the elderly group and 21.6 (95% CI; 18.0–29.0) months in the nonelderly group. OS was significantly longer in the nonelderly group (log-rank test, p = 0.021).

PFS was 8.4 (95% CI; 5.1–11.7) months in the elderly group, and 12.7 (95% CI 9.5–16.7) months in the nonelderly group (p = 0.078); PFS tended to be longer in the nonelderly group.

V. Prognostic factors and effect on OS and PFS in the elderly group

Results of univariate analysis of prognostic factors are shown in Table 5. RPA score (IV and V versus VI; p < 0.01) was the prognostic factors for OS. Median OS was 15.1 months in the age 65–69 bracket, 18.5 months in the age 70–74 bracket, and 15.3 months in the age 75-years-and-over bracket.

RPA score (IV and V versus VI) seemed to be a prognostic factor for PFS with borderline significance (p = 0.05). Extent of resection (gross total removal versus partial removal and biopsy), KPS, and *MGMT* promoter methylation were poorly correlated with PFS. Median PFS was 5.3 months in the age 65–69 bracket, 9.8 months in the age 70–74 bracket, and 8.9 months in the age 75-years-and-over bracket. Like OS, PFS did not differ significantly between the age brackets within the elderly group.

Table 5 Prognostic factors for OS and PFS

	N	Median OS (months)	p value	Median PFS (months)	p value
Sex					
Male	16	15.1	0.83	6	0.93
Female	11	16.2		8.9	
Age					
≥ 75	7	15.3	0.72	8.9	0.41
70–74	11	18.5		9.8	
65–70	9	15.1		5.3	
Extent of resection					
GTR	6	n.r.	0.57	8.9	0.31
PR, biopsy	21	15.1		6	
KPS					
≥ 70	19	15.3	0.63	8.4	0.95
< 70	8	12.9		9.8	
RPA score					
IV–V	24	16.2	< 0.01*	8.9	0.05
VI	3	9.3		3.4	
MGMT					
Methylated	8	12.9	0.7	5.3	0.33
Unmethylated	11	18.5		9.8	
Adverse event (Grade 4)					
(+)	8	15	0.15	8.4	0.75
(–)	19	15.3		8.9	

*Significant value. GTR: gross total removal, KPS: Karnofsky performance status, *MGMT*: O6-methylguanine methyltransferase, n.r.: not reached, OS: overall survival, PFS: progression-free survival, PR: partial removal, RPA: recursive partitioning analysis.

Discussion

In this study, an increased incidence of Grade 4 adverse events and cognitive dysfunction was observed in the elderly patients especially during the concomitant course. Overall Grade 3 and 4 hematologic toxicity during concomitant and adjuvant chemotherapy with TMZ in the elderly patients was reported to range from 6% to 18% and 10% to 22%, respectively.[5,6,9,10] Meanwhile, the present study showed a higher incidence of overall Grade 3 and 4 hematologic toxicity in elderly patients; 37% and 36% during the concomitant and adjuvant courses, respectively. Unexpectedly, this higher rate of hematologic toxicity was not specific to elderly patients, and the incidence of overall Grade 3 and 4 hematologic toxicity in the nonelderly group was